



**HAL**  
open science

# New atrio-ventricular indices derived from conventional cine MRI correlate with functional capacity in patients with asymptomatic primary mitral regurgitation

Perrine Marsac, Thomas Wallet, Alban Redheuil, Moussa Gueda Moussa, Jérôme Lamy, Vincent Nguyen, Etienne Charpentier, Nadjib Hammoudi, Emilie Bollache, Nadja Kachenoura

## ► To cite this version:

Perrine Marsac, Thomas Wallet, Alban Redheuil, Moussa Gueda Moussa, Jérôme Lamy, et al.. New atrio-ventricular indices derived from conventional cine MRI correlate with functional capacity in patients with asymptomatic primary mitral regurgitation. *Scientific Reports*, 2024, 14 (1), pp.21429. 10.1038/s41598-024-71563-4 . hal-04697427

**HAL Id: hal-04697427**

**<https://hal.science/hal-04697427>**

Submitted on 16 Sep 2024

**HAL** is a multi-disciplinary open access archive for the deposit and dissemination of scientific research documents, whether they are published or not. The documents may come from teaching and research institutions in France or abroad, or from public or private research centers.

L'archive ouverte pluridisciplinaire **HAL**, est destinée au dépôt et à la diffusion de documents scientifiques de niveau recherche, publiés ou non, émanant des établissements d'enseignement et de recherche français ou étrangers, des laboratoires publics ou privés.



OPEN

## New atrio-ventricular indices derived from conventional cine MRI correlate with functional capacity in patients with asymptomatic primary mitral regurgitation

Perrine Marsac<sup>1</sup>, Thomas Wallet<sup>2</sup>, Alban Redheuil<sup>3</sup>, Moussa Gueda Moussa<sup>1</sup>, Jérôme Lamy<sup>4</sup>, Vincent Nguyen<sup>1</sup>, Etienne Charpentier<sup>3</sup>, Nadjib Hammoudi<sup>2</sup>, Emilie Bollache<sup>1</sup> & Nadjia Kachenoura<sup>1</sup>✉

Mitral regurgitation (MR) is associated with morphological and functional alterations of left atrium (LA) and ventricle (LV), possibly inducing LA–LV misalignment. We aimed to: (1) characterize angulation between LA and mitral annulus from conventional cine MRI data and feature-tracking (FT) contours, (2) assess their associations with functional capacity in MR patients, as assessed by oxygen consumption (peak-VO<sub>2</sub>) and minute ventilation to carbon dioxide production (VE/VCO<sub>2</sub>) slope, in comparison with MRI LA/LV strain indices. Thirty-two asymptomatic primary MR patients (56 [40; 66] years, 12 women) underwent cardiac MRI resulting in LA/LV conventional FT-derived strain indices. Then, end-diastolic angles were derived from FT LA contours: (1)  $\alpha$ , centered on the LA centre of mass and defined by mitral valve extremities, (2)  $\gamma$ , centered on the mitral ring anterior/lateral side, and defined by LA centre and the other extremity of the mitral ring. Cardiopulmonary exercise testing with simultaneous echocardiography were also performed; peak-VO<sub>2</sub> and VE/VCO<sub>2</sub> slope were measured. While peak-VO<sub>2</sub> and VE/VCO<sub>2</sub> slope were not correlated to LA/LV strains, they were significantly associated with angles ( $\alpha$ :  $r = 0.50$ ,  $p = 0.003$  and  $r = -0.52$ ,  $p = 0.003$ ;  $\gamma$ :  $r = -0.53$ ,  $p = 0.002$  and  $r = 0.52$ ,  $p = 0.003$ ; respectively), independently of age and gender ( $R^2 \geq 0.29$ ,  $p \leq 0.03$ ). In primary MR, the new LA/mitral annulus angles, computed directly from standard-of-care MRI, are better correlated to exercise tolerance than conventional LA/LV strain.

Primary mitral valve regurgitation (MR) is the second most frequent valvular heart disease in Europe<sup>1</sup>. Due to volume overload, MR induces morphological and functional changes in both left ventricle (LV) and left atrium (LA), and the enlargement of left heart chambers in chronic primary MR occurs progressively even before symptoms appearance<sup>2</sup>. Therefore, MR precise characterization and severity assessment along with evaluation of LV and LA involvement are essential to help patient management and therapeutic or surgical decision-making<sup>3</sup>.

Imaging modalities play a major role in the exploration of patients with MR. Indeed, echocardiography is the first intent and an effective method for MR quantification. Furthermore, recent cardiac MRI studies highlighted that MRI phase-contrast and volumetric measures could provide additional information and may achieve higher performances in MR severity assessment and outcome prediction<sup>4,5</sup>.

Beyond the ability of MRI to accurately assess heart chamber volumes and myocardial fibrosis, the use of feature tracking (FT) on conventional cine images, without any extra acquisition, is evolving for the exploration of both LV<sup>6,7</sup> and LA<sup>8–11</sup> function in various disease conditions including MR<sup>12,13</sup>. Such simultaneous LA and LV exploration on cine long axis MRI images can provide further investigations into LA and LV misalignment and mitral annulus inclination, without extra complex analysis since FT time-resolved contours are readily available.

<sup>1</sup>Sorbonne Université, Inserm, CNRS, Laboratoire d'Imagerie Biomédicale, LIB, 15 rue de l'école de médecine, 75006 Paris, France. <sup>2</sup>Sorbonne Université, ACTION Study Group, INSERM UMRS\_1166, Institut de Cardiologie, Hôpital Pitié-Salpêtrière (AP-HP), Paris, France. <sup>3</sup>Hôpital Universitaire Pitié-Salpêtrière, Unité d'Imagerie Cardiovasculaire et Thoracique (ICT), Paris, France. <sup>4</sup>Hôpital Européen Georges-Pompidou, Cardiovascular Research Center (PARCC, Inserm U970), Paris, France. ✉email: najia.kachenoura@inserm.fr

As such, horizontal inclination of the mitral annular plane has been recently shown in patients with MR and atrial dilatation, and such horizontal tilt decreased with surgical plication while LA size was lower<sup>14</sup>. Another study<sup>15</sup> proposed an LA-LV angulation index, which was described as a measure of LA and LV remodelling and predicted by LV and LA size and mitral regurgitation.

Accordingly, in the present study, we took advantage of LV and LA FT time-resolved contours derived from MRI long axis images: (1) to define new LA/LV angles based on mitral inclination and LA/LV remodelling; (2) to compare associations of such angle indices and conventional FT-derived LV and LA strain indices with MRI-independent indicators of exercise tolerance, including peak  $\text{VO}_2$  oxygen consumption and minute ventilation to carbon dioxide production slope as a reflect of ventilatory efficiency, in patients with asymptomatic chronic primary MR and preserved ejection fraction.

## Materials and methods

### Study population and data acquisition

This retrospective study included 32 patients (median age: 56 [40; 66] years;  $n = 12$ , 38% women) with asymptomatic primary MR and preserved LV ejection fraction (LVEF), who underwent exercise transthoracic echocardiography (TTE) combined with gas exchange measurements and cardiac MRI. Based on the European Society of Cardiology guidelines<sup>3</sup>, asymptomatic was defined as a patient who has not reported exercise intolerance as assessed using New York Heart Association (NYHA) classification. Hence, we only included Class I NYHA patients. While TTE and MRI were performed within a median delay of 22 [5; 62] days, more than half of patients underwent these explorations within the same month ( $n = 18$ , 56%). Exclusion criteria were: Class I recommendation of mitral surgery (symptoms, TTE LVEF  $\leq 60\%$  or LV systolic diameter  $\geq 40$  mm), aortic regurgitation, prior surgical interventions, known coronary artery disease, congenital cardiomyopathy or inability to perform exercise. This clinical study was carried out according to the principles outlined in the Declaration of Helsinki. Exercise TTE combined with gas exchange measurements and MRI are performed in routine practice in asymptomatic MR patients, a written informed consent for such investigations was signed by all participants. The retrospective use of these data was allowed by the Research Ethics Committee of Sorbonne Université under the reference CER-2021-095. This study complies with the reference methodology (MR004) of the French National Commission for Informatics and Liberties. According to the French national legislation, the use of retrospective data is rendered legal through such MR004, which provides the ethics approval. MRI data of additional 17 healthy volunteers with similar age and gender balance to the MR patients were also selected from control groups of previous local databases (Clinical Trials #NCT02517944, NCT02059538).

TTE proximal isovelocity surface area (PISA) method was used to measure effective regurgitant orifice area (EROA) as well as regurgitant volume. Conventional LV forward stroke volume and the ratio of mitral inflow to aortic outflow velocity–time integrals (VTI) were also assessed by pulsed wave Doppler<sup>16</sup>. After baseline evaluation, a maximal symptom-limited cardiopulmonary exercise testing with simultaneous echocardiography (Vivid E9, General Electric, Horten, Norway) was performed on semi-supine cycle ergometer (Ultra Koch, Le Haillan, France) using a standardized incremental ramp protocol (start with 10 W, followed by increments of 10–20 W per min depending on patient predicted maximal exercise capacity)<sup>17,18</sup>; maximal workload as well as maximal and % predicted maximal heart rate were reported. Oxygen consumption ( $\text{VO}_2$ ), minute ventilation (VE), and carbon dioxide production ( $\text{VCO}_2$ ) were assessed throughout the examination (CARDIOVIT CS-200, Schiller, Baar, Switzerland). Peak  $\text{VO}_2$  was expressed as the highest  $\text{VO}_2$  measurement obtained during exercise and was indexed to body weight.  $\text{VE}/\text{VCO}_2$  slope was calculated via least squares linear regression at peak. Peak respiratory exchange ratio (RER), as an indicator of maximal exercise effort, was defined as the highest  $\text{VCO}_2/\text{VO}_2$  ratio obtained during exercise. Exercise capacity was also expressed as percentage of predicted peak  $\text{VO}_2$  according to age and sex. Finally, peak tricuspid regurgitation velocity (TRV) was recorded as an index of systolic pulmonary artery pressure (SPAP) at rest as well as at low exercise (30 W) and peak exercise levels.

MRI was performed on a 1.5 T scanner (Aera, Siemens, Erlangen, Germany). Standard cine images were obtained using a balanced steady-state free precession (SSFP) sequence with multiple breath-holds and ECG gating. Short- and long-axis (2- and 4-chamber views) SSFP imaging was performed with the following acquisition parameters, reported as median value (minimal–maximal values): echo time (TE): 1.2 (0.9–1.4) ms; repetition time (TR): 2.8 (2.1–3.1) ms; temporal resolution: 38 (23–54) ms; 25 reconstructed images per cardiac cycle; flip angle: 53 (50–62)°; acquisition matrix: (128–256) × (66–256); pixel size: 1.5 (1.2–3.2) mm; slice thickness: 6 (4–8) mm. Furthermore, a 2D phase-contrast (PC) sequence was acquired in a cross-sectional slice perpendicular to the ascending aorta at the level of the pulmonary trunk bifurcation, under breath-hold using ECG gating and the following acquisition parameters: TE: 3.3 (2.5–4.3) ms; TR: 5.5 (4.6–6.5) ms; temporal resolution: 16 (10–21) ms; 60 reconstructed images per cardiac cycle; flip angle: 20°; acquisition matrix: 192 × (97–119); pixel size: 2.1 (1.8–2.6) mm; slice thickness: 6 mm; encoding velocity: 150 cm/s.

### MRI image analysis

LA and LV volumes were conventionally measured using QMass software (Medis Medical Imaging, Leiden, The Netherlands). LV end-diastolic and end-systolic volumes and mass were estimated from short-axis cine images through tracing of endocardial and epicardial contours from base to apex at end-diastole and end-systole. Maximal and minimal LA volumes were estimated from 2- and 4-chamber views while using the area-length method. LV stroke volume as well as LV and LA ejection fractions were further calculated. Cardiac volumes and mass were indexed to body surface area. Aortic ejection volume was measured using PC images and a previously described and validated semi-automated delineation of ascending aortic wall borders throughout the cardiac cycle<sup>19</sup>; finally, common MRI-derived mitral regurgitation volume was computed as LV stroke volume—PC images-derived aortic ejection volume<sup>20</sup>.

Cine images were further analysed using an in-house FT software (CardioTrack, LIB, Sorbonne Université) widely validated for myocardial strain estimation on both human<sup>6,8,11,21,22</sup> and animal<sup>23,24</sup> MRI data. Briefly, after endocardial (LA, LV) and epicardial (LV) contours initialization on a single temporal phase, tracking was performed on the adjacent time-phases successively toward the beginning and the end of the cardiac cycle. For such tracking, a region of interest is defined around each point of the initial contour. Then a map with the cross-correlation values between this region and its spatial neighbourhood on the next time phase is calculated. This cross-correlation map is weighted with additional maps derived from image properties and constraints related to physiological knowledge regarding contractile function, as described in Ref.<sup>6</sup>. FT contours were used to estimate time-resolved strain curves for both the LV, as an average of epicardial and endocardial strain, and the LA. Then LV peak systolic circumferential and longitudinal strains, as well as reservoir, conduit and booster LA longitudinal strains, which were averaged from 2- and 4-chamber view measures, were derived.

Finally, FT long-axis contours derived from both 2- and 4-chamber views were further used to estimate LA to mitral annulus angulation (Fig. 1) through the two following angles:  $\alpha$  was the angle centered on the LA centre of mass and defined by mitral valve extremities;  $\gamma$  was the angle centered on the anterior/lateral side of the mitral annulus and defined by the LA centre of mass and the mitral annulus plane. End-diastolic angles were finally extracted from time-resolved curves and maximal value between 2- and 4-chamber views was collected.

Reproducibility of end-diastolic  $\alpha$  and  $\gamma$  was assessed in the 17 healthy individuals after analysis of MRI data by 2 independent users (PM and MGM).

### Statistical analyses

We determined sample size with a power calculation; indeed, in order to detect a correlation above 0.50 (Pearson's coefficient) between the primary end-point MRI angle indices and indicators of exercise capacity with 80% power and 5% alpha level, a sample of 24 patients is required. Continuous variables were expressed as median and interquartile range. Patients were divided into subgroups according to exercise capacity, as defined by peak  $\text{VO}_2$  tertiles. Comparisons across peak  $\text{VO}_2$  and control groups were performed using a Kruskal–Wallis test for continuous variables and Fisher's exact test for discrete variables. Associations of the proposed angles and conventional echocardiographic TRV as well as MRI LV and LA volume and strain indices with peak  $\text{VO}_2$ , % age-predicted peak  $\text{VO}_2$  and  $\text{VE}/\text{VCO}_2$  slope as prognostic and MRI-independent parameters of functional capacity in MR patients<sup>25</sup>, were studied using linear regressions. Pearson's correlation coefficients were reported. For significant relationships, further adjustment for age and sex was performed using multivariate models. Finally, inter-operator reproducibility was assessed through intraclass correlation coefficient. Tests were two-tailed and statistical significance was set to a p value < 0.05. Statistical analyses were carried out using JMP software (Cary, NC, USA).

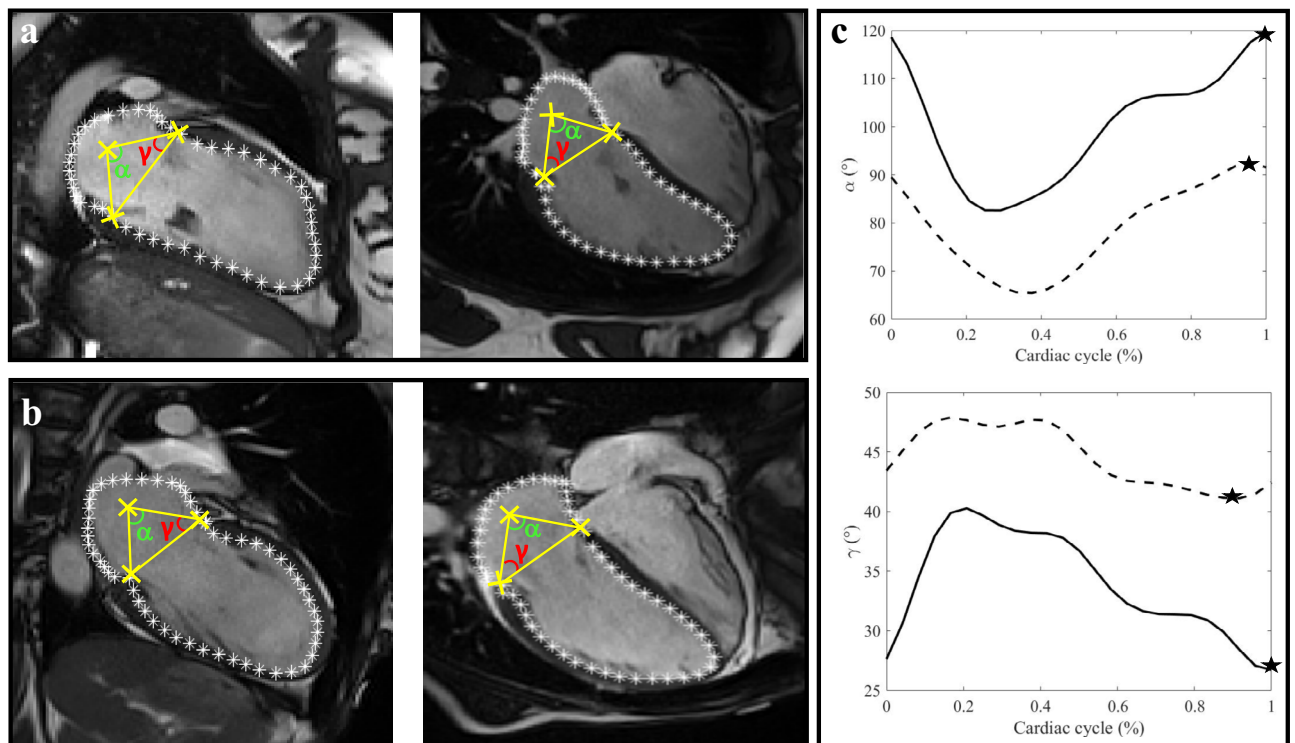


**Fig. 1.** LA-mitral annulus angles extracted from FT-derived contours on cine SSFP long-axis images. 2- (left) and 4- (right) chamber view cine SSFP image at diastolic phase for a patient with high exercise capacity (a) and low exercise capacity (b). (c) Angle curves with end-diastolic values (black filled stars) of patient with high (solid line) and low (dashed line) exercise capacity.

## Results

Table 1 summarises patient and control characteristics along with patient TTE parameters, exercise testing measures as well as MRI regurgitant volume, LV and LA volumes, strain and angle indices according to  $VO_2$  tertiles. As per study design, healthy volunteers and patients had similar age ( $p=0.19$ ) and proportion of men ( $p=0.71$ ). All included patients performed maximal exercise effort as reflected by RER values. Five patients (16%) had atrial fibrillation (AF), among which 4 had paroxysmal AF and were investigated in sinus rhythm, while the last patient had permanent AF but had a heart rate of 68 bpm at rest so imaging quality was not altered by tachycardia. All patients had a heart rate below 87 bpm during MRI. There were no significant differences across groups in age, BMI and gender. Although regurgitant volume whether assessed using echocardiography or MRI, as well as TTE EROA, LV forward stroke volume and mitral to aortic VTI ratio were similar across the 3  $VO_2$  tertile groups, EROA, forward stroke volume and mitral/aortic VTI ratio were higher in the second group. TRV

	1st $VO_2$ tertile	2nd $VO_2$ tertile	3rd $VO_2$ tertile	Controls	p-value
Peak $VO_2$ (mL/kg/min)	Peak $VO_2 < 25$	$25 \leq$ Peak $VO_2 < 29$	Peak $VO_2 \geq 29$	–	
n	11	10	11	17	
Basic characteristics					
Age (years)	63 [48; 71]	62 [39; 67]	50 [37; 60]	50 [36; 57]	0.18
BMI (kg/m <sup>2</sup> )	25.9 [23.8; 30.6]	23.6 [21.1; 25.2]	22.4 [19.2; 26]	24.7 [22.7; 27.5]	0.11
Males (N)	6	6	8	10	0.84
Heart rate during MRI (bpm)	61 [55; 69]	68 [57.8; 72.3]	57 [50; 65]	63 [57.5; 68]	0.29
TTE parameters and exercise testing characteristics					
Effective regurgitant orifice area (cm <sup>2</sup> )	0.32 [0.22; 0.41]	0.43 [0.36; 0.72]	0.30 [0.22; 0.59]	–	0.13
Forward stroke volume (mL)	73.7 [69.1; 86.5]	78.5 [71.8; 101]	72.3 [60.8; 108]	–	0.71
Regurgitant volume (mL)	60.2 [29.9; 70.0]	59.6 [43.5; 124.1]	39.9 [31.2; 80.3]	–	0.33
Mitral/aortic VTI ratio	1.16 [0.96; 1.37]	1.41 [1.25; 1.51]	1.32 [1.10; 1.79]	–	0.27
Rest TRV (m/s)	2.8 [2.4; 3.1]	2.5 [2.4; 2.8]	2.3 [2.0; 2.3]	–	<b>0.007</b>
Low exercise level TRV (m/s)	3.1 [3.0; 3.3]	3.0 [2.7; 3.4]	2.7 [2.6; 2.9]	–	0.05
Peak exercise TRV (m/s)	3.4 [2.9; 3.6]	3.6 [3.3; 3.6]	3.4 [2.9; 3.6]	–	0.58
Maximal workload (W)	129 [90; 181]	145 [116; 204]	186 [162; 229]	–	0.08
Maximal heart rate (bpm)	150 [143; 161]	152 [138; 164]	160 [156; 172]	–	0.21
% predicted maximal heart rate (%)	92 [88; 95]	92 [87; 96]	94 [90; 98]	–	0.53
RER at peak exercise	1.32 [1.22; 1.38]	1.29 [1.22; 1.45]	1.25 [1.07; 1.38]	–	0.39
Peak $VO_2$ (mL/kg/min)	21.3 [16.4; 24.0]	27 [26.1; 27.6]	30.4 [30; 34.5]	–	<b>&lt;0.0001</b>
% age-predicted peak $VO_2$ (%)	79 [70; 93]	100 [76; 115]	102 [94; 105]	–	<b>0.008</b>
VE/ $VCO_2$ slope	25.0 [24.8; 28.4]	23.4 [21.2; 26.4]	22.7 [20.0; 22.7]	–	<b>0.002</b>
MRI parameters					
Regurgitant volume (mL)	62.9 [40.8; 75.8]	43.0 [34.8; 59.9]	47.9 [36.4; 64.2]	–	0.56
Indexed LV mass (g/m <sup>2</sup> )	47.4 [43.1; 54.7]	50.6 [48.4; 55.6]	48.4 [44.5; 59.5]	49.0 [45.5; 54.9]	0.57
Indexed LVEDV (mL/m <sup>2</sup> )	101 [89; 114]	113 [99; 127]	122 [95; 144]	84 [75; 92]	<b>&lt;0.0001</b>
Indexed LVESV (mL/m <sup>2</sup> )	35 [30; 41]	41 [33; 49]	43 [35; 54]	34 [28; 38]	<b>0.02</b>
Indexed LV stroke volume (mL/m <sup>2</sup> )	67 [59; 70]	71 [65; 86]	69 [63; 88]	48 [42; 57]	<b>&lt;0.0001</b>
LVEF (%)	64 [60; 70]	64 [61; 68]	63 [57; 66]	60 [55; 67]	0.21
Indexed LA max volume (mL/m <sup>2</sup> )	59 [52; 71]	82 [62; 105]	70 [52; 81]	39 [34; 45]	<b>&lt;0.0001</b>
Indexed LA min volume (mL/m <sup>2</sup> )	31 [21; 39]	43 [30; 73]	35 [23; 40]	15 [14; 17]	<b>&lt;0.0001</b>
LAEF (%)	49 [47; 53]	48 [44; 60]	50 [47; 55]	60 [57; 63]	<b>0.0001</b>
LV circumferential strain (%)	–18.7 [–21.2; –18.2]	–19.5 [–23.1; –18.4]	–18.5 [–20.0; –15.8]	–20.5 [–21.4; –18.3]	0.22
LV longitudinal strain (%)	–20.7 [–21.8; –19.0]	–21.0 [–23.1; –18.0]	–18.9 [–19.8; –18.2]	–20.6 [–21.4; –18.5]	0.43
LA reservoir longitudinal strain (%)	25.7 [23.5; 31.0]	24.5 [15.2; 29.3]	24.1 [19.0; 27.1]	42.3 [36.5; 45.7]	<b>&lt;0.0001</b>
LA conduit longitudinal strain (%)	15.7 [11.4; 20.1]	15.3 [12.7; 18.5]	15.8 [11.1; 16.8]	21.6 [16.8; 24.4]	<b>0.01</b>
LA booster longitudinal strain (%)	12.1 [8.5; 13.5]	7.6 [3.8; 12.0]	8.9 [7.7; 10.8]	21.3 [18.0; 24.6]	<b>&lt;0.0001</b>
End-diastolic $\alpha$ angle (°)	84.5 [76.4; 92.5]	86.8 [83.2; 99.6]	99.0 [92.6; 108.5]	95.8 [92.8; 100.2]	<b>0.004</b>
End-diastolic $\gamma$ angle (°)	45.5 [41.1; 51.9]	42.9 [37.2; 48.7]	37.7 [34.4; 40.5]	41.7 [40.3; 45.0]	<b>0.01</b>

**Table 1.** Patient and control characteristics, TTE, functional capacity parameters and MRI indices according to  $VO_2$  tertiles. Values are shown as median [interquartile range]. Significant values are in bold. *BMI* body mass index, *LA* left atrium, *LV* left ventricle, *LVEDV* LV end-diastolic volume, *LVESV* LV end-systolic volume, *LVEF* LV ejection fraction, *LAEF* LA ejection fraction, *RER* respiratory exchange ratio, *TTE* transthoracic echocardiography, *TRV* tricuspid regurgitation velocity, *VE* minute ventilation, *VCO<sub>2</sub>* carbon dioxide production, *VTI* velocity–time integral, *VO<sub>2</sub>* oxygen consumption rate, *bpm* beats per minute.

at rest was gradually and significantly higher in patients with lower peak  $\text{VO}_2$ , and increased during exercise at low and then peak levels in all 3 groups. Finally, as expected, % age- and sex-predicted peak  $\text{VO}_2$  was significantly lower and  $\text{VE}/\text{VCO}_2$  slope was significantly higher across groups as peak  $\text{VO}_2$  decreased.

Indexed LV mass and LA volumes were higher in the second  $\text{VO}_2$  group, but only indexed LA maximal volume reached significant difference across the 3 patient groups ( $p = 0.02$ ). Indexed LV volumes increased gradually across  $\text{VO}_2$  patient groups but such difference did not reach statistical significance ( $p \geq 0.05$ ). As per inclusion criteria, LV ejection fraction (LVEF) and LA ejection fraction (LAEF) lied within normal ranges in all groups, and LV and LA strains were equally distributed across  $\text{VO}_2$  groups, except for a light drop in LA booster strain in the second group, which however did not reach statistical significance ( $p = 0.14$ ). As expected, healthy volunteers had significantly lower LV and LA volumes, as well as higher LA ejection fraction and strains. Finally, regarding LA angle indices, a gradual increase in  $\alpha$  angle and decrease in  $\gamma$  angle were observed across groups, reaching statistical significance for all indices ( $p \leq 0.01$ ). Of note, measurement of end-diastolic angle indices was reproducible, as reflected by high intraclass correlation coefficients = 0.81 for  $\alpha$  and = 0.78 for  $\gamma$ .

In univariate analyses, peak  $\text{VO}_2$  and  $\text{VE}/\text{VCO}_2$  slope were significantly correlated to TRV measured using TTE at rest ( $r = -0.41$ ,  $p = 0.03$  and  $r = 0.55$ ,  $p = 0.004$ , respectively) and low exercise level ( $r = -0.44$ ,  $p = 0.02$  and  $r = 0.51$ ,  $p = 0.009$ , respectively), but not at peak exercise level ( $p = 0.89$  and  $p = 0.39$ , respectively). Importantly, while peak  $\text{VO}_2$  and  $\text{VE}/\text{VCO}_2$  slope were not significantly correlated to any of the MRI-derived LV and LA strain indices, they were significantly associated with angle indices (Fig. 2), resulting in overall stronger and higher associations with  $\alpha$  ( $r = 0.50$ ,  $p = 0.003$  and  $r = -0.52$ ,  $p = 0.003$ , respectively) and with  $\gamma$  ( $r = -0.53$ ,  $p = 0.002$  and  $r = 0.52$ ,  $p = 0.003$ , respectively). The following relationships obtained with TRV and angle indices were independent of age and sex: rest TRV (peak  $\text{VO}_2$ :  $R^2 = 0.39$ ,  $p = 0.007$  and  $\text{VE}/\text{VCO}_2$  slope:  $R^2 = 0.37$ ,  $p = 0.02$ ), low exercise TRV (peak  $\text{VO}_2$ :  $R^2 = 0.31$ ,  $p = 0.03$ ), end-diastolic  $\alpha$  (peak  $\text{VO}_2$ :  $R^2 = 0.45$ ,  $p = 0.0008$  and  $\text{VE}/\text{VCO}_2$  slope:  $R^2 = 0.31$ ,  $p = 0.02$ ), and end-diastolic  $\gamma$  (peak  $\text{VO}_2$ :  $R^2 = 0.43$ ,  $p = 0.001$  and  $\text{VE}/\text{VCO}_2$  slope:  $R^2 = 0.29$ ,  $p = 0.03$ ). Of note, among volume indices, the only significant correlates of peak  $\text{VO}_2$  and  $\text{VE}/\text{VCO}_2$  slope were LV volumes (indexed LV end-diastolic volume (LVEDV):  $r = 0.45$ ,  $p = 0.009$  and  $r = -0.49$ ,  $p = 0.007$ , respectively);

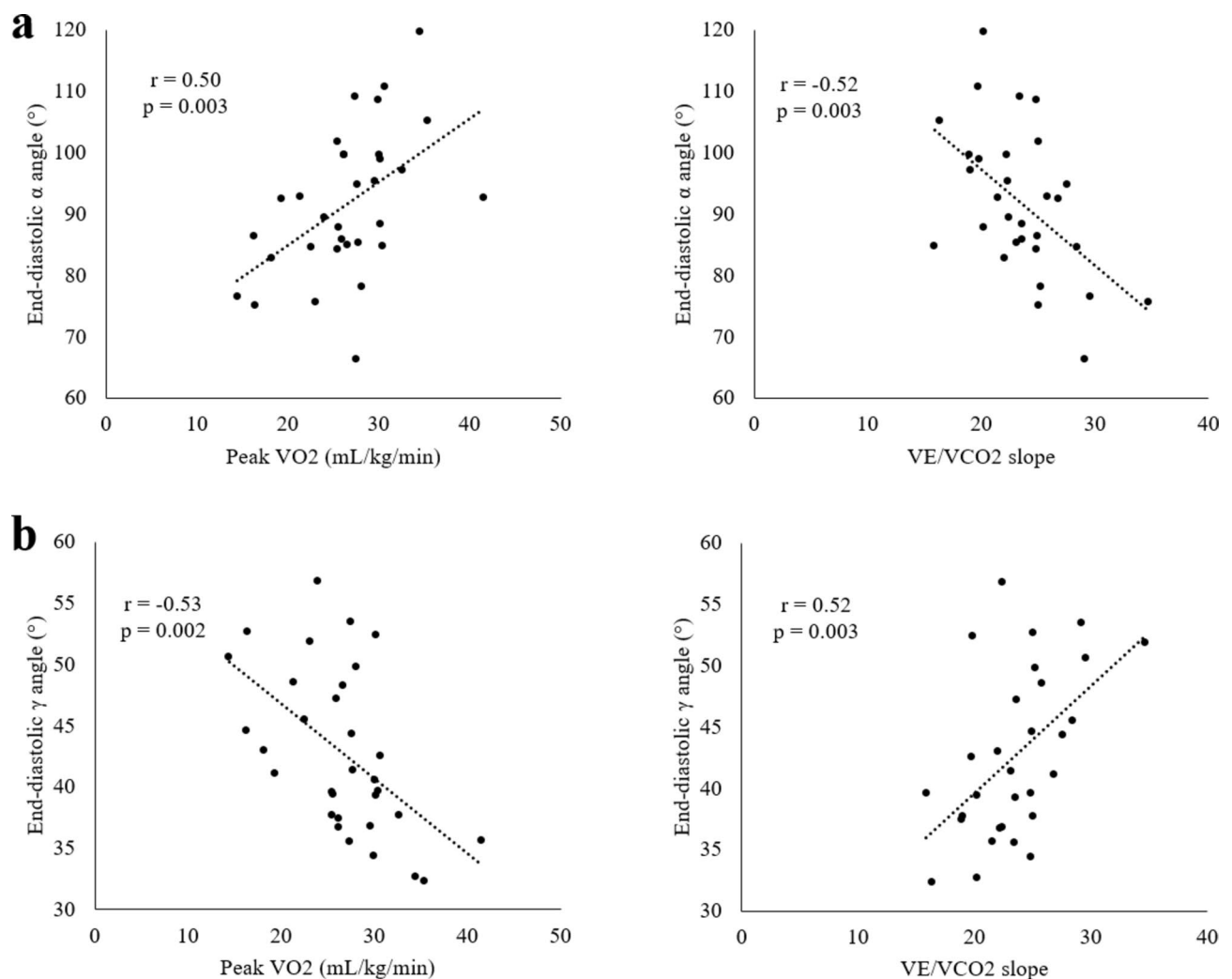


**Fig. 2.** Linear regressions of peak  $\text{VO}_2$  and  $\text{VE}/\text{VCO}_2$  slope with end-diastolic angle indices. (a) End-diastolic LA  $\alpha$  angle. (b) End-diastolic LA  $\gamma$  angle.

indexed LV end-systolic volume (LVESV):  $r = 0.45$ ,  $p = 0.01$  and  $r = -0.51$ ,  $p = 0.004$ , respectively; indexed LV stroke volume:  $r = 0.37$ ,  $p = 0.04$  and  $r = -0.37$ ,  $p = 0.04$ , respectively). However, these associations were no longer significant after adjustment for sex and age. Finally, no significant relationship was obtained against % age- and sex-predicted peak  $\text{VO}_2$ .

## Discussion

In the present study, we proposed indices related to LA-mitral annulus angulation, which can be directly quantified from standard-of-care MRI cine images combined with feature-tracking which is commonly used to derive myocardial strain. We demonstrated in patients with asymptomatic primary MR and preserved LVEF, that peak  $\text{VO}_2$  and  $\text{VE}/\text{VCO}_2$  slope, which are standard measures of exercise capacity and ventilatory efficiency linked to prognosis<sup>25–28</sup>, were associated with angle indices, independently of age and gender. In contrast, peak  $\text{VO}_2$  and  $\text{VE}/\text{VCO}_2$  slope were not significantly correlated to any of the conventional LV and LA strain indices. An advantage of such mitral annulus angulation indices is that they do not require additional MRI scan or analysis time.

MRI strains in our study were in agreement with previous speckle tracking echocardiographic studies. Indeed, Mentias et al. and Alashi et al. reported LV longitudinal strain mean values of  $-21.5 \pm 2.0$  and  $-20.6 \pm 2\%$ , respectively, in patients with primary MR and preserved LVEF before surgery<sup>29,30</sup>. Yang et al. further studied 136 patients with severe primary MR and preserved LVEF, and found that LA peak reservoir strain was  $25.86 \pm 9.89\%$ <sup>31</sup>, which is in line with our findings. Ahmed et al. measured LV strain rates of patients with severe MR using tagged MRI<sup>32</sup> but to the best of our knowledge, no studies previously investigated strain measurement using cine SSFP images in patients with primary MR. Indeed FT has been used in recent MRI studies rather to perform slice tracking and enhance mitral flow measurements in MR patients than to specifically evaluate strain<sup>33</sup>.

While there was a drop in LA strains in MR patients as compared to controls, LV strain values were in a normal range despite LV dilatation in our MR patients. Indeed, loading conditions which are affected by the large regurgitant volume in MR patients are associated with LV and LA enlargement. Such dilatation is compensated by mechanical adaptation of left heart chambers, according to Frank-Starling law<sup>34</sup>, maintaining a certain level of myocardial strains. This probably partially explains why strain was not a significant correlate of peak  $\text{VO}_2$  and  $\text{VE}/\text{VCO}_2$  slope in this study.

LV shape has been widely associated to exercise capacity<sup>35</sup>, beyond LV function<sup>36</sup>. This is in line with our findings, where LV volume was significantly associated to peak  $\text{VO}_2$  and  $\text{VE}/\text{VCO}_2$  slope. Such LV remodelling in asymptomatic MR patients was required to maintain sufficient stroke volume and reasonable exercise capacity. The newly proposed angle indices, which are driven by both LA geometry and mitral annulus shape and angulation, were found to be strongly and independently associated with exercise capacity-related peak  $\text{VO}_2$ . Interestingly, LA to mitral annulus angles were further found to be significantly and independently correlated with  $\text{VE}/\text{VCO}_2$  slope, which reflects ventilatory efficiency. Indeed, elevated  $\text{VE}/\text{VCO}_2$  slope indicates abnormal ventilatory response to exercise, that could be explained by elevation of filling or pulmonary pressures, increase in dead space, and reduction of pulmonary flow. This parameter was previously found to be associated with clinical outcomes and prognosis in heart failure, hypertrophic cardiomyopathy<sup>37</sup>, and in valvular heart disease<sup>28,38</sup>. Such  $\text{VE}/\text{VCO}_2$  slope-related findings are consistent with the revealed significant correlations with peak  $\text{VO}_2$ .

Chronic severe MR induces volume overload that progressively leads to compensatory mechanisms from LA and LV, with a chronic remodelling process and enlargement of left cardiac chambers. Eventually, compensatory adaptation fails, leading to deleterious LA and LV dilatation and LV dysfunction. However, transition from a compensated remodelling to decompensated stage of MR remains unclear. LA and LV remodelling includes dilatation but also further changes in heart shape and geometry as well as myocardial and annulus stiffness, which may induce annular tilt in the course of cardiac cycle. LA to LV angulation indices, as assessed from Computed Tomographic Angiography, have been previously described as new markers of cardiac remodelling, and were found to be correlated with MR severity, suggesting that they could be a complementary parameter of cardiac remodelling in chronic MR<sup>15</sup>. In the current study, we proposed new LA to mitral annulus angulation from standardized MRI left heart views and automated myocardial tracking, which integrates both LA and LV dilatation and reshape, as well as changes in mitral annulus dimensions and angulation, which are important components in primary MR. Such remodelling-related angle indices might complement flow and volume indices for MR severity grading, and ultimately help distinguish compensated remodelling from decompensated stage and thus improve prognosis evaluation in chronic primary MR.

Systolic pulmonary artery pressure (SPAP) is an important parameter in chronic MR. Indeed, it has been found to be associated with prognosis, especially mortality after mitral surgery<sup>39</sup>. Exercise-induced pulmonary hypertension (ExpHT), which was notably demonstrated to predict cardiovascular outcome in chronic MR, is also a valuable parameter<sup>40</sup>. Since echocardiographic SPAP assessment during exercise can be challenging due to a loss in Doppler signal, peak TRV was recorded during our TTE protocols as an index of SPAP. We found that it was significantly and independently correlated to peak  $\text{VO}_2$  both at rest and during low exercise, albeit to a lesser degree than our MRI angle indices.

Our study has some limitations. First, our population was small. However, it is well phenotyped, and our primary objective was to perform a head-to-head comparison between the newly proposed angle indices and conventional volumetric and strain parameters, in regard to patients exercise capacity. Also, this was a cross-sectional study thus we did not have any follow-up data to assess the prognostic value of our new angle indices, as well as their additive performance to SPAP or ExpHT evaluations. In addition, the fact that our LA-mitral annulus angles are measured from 2-dimensional images, which are further centred on the left ventricle, could be viewed as a limitation. However, in a generalizability purpose, our goal was to propose indices readily available from conventional and highly standardized cine images that are acquired during any cardiac MRI protocol. Associations of angle indices with  $\text{VO}_2$  and  $\text{VE}/\text{VCO}_2$  slope attest on the consistency of our measures. To date,

there is no 3D + t cine MRI sequence easily usable in clinical routine to afford 3D angles estimation, hence we designed our study rational based on existing standardized sequences. The emergence of such sequences in the near future will strengthen true angle estimates. Exercise TTE and MRI assessments were not performed on the same day. Indeed, our data were collected within a real-life setting in the course of clinical routine protocols, where TTE was performed first and MRI was achieved while considering pragmatic constraints, allowing a maximal interval of around 6 months. We did our best all along inclusions to ensure that both examinations were carried out within the shortest interval, and more than half of patients underwent these explorations within the same month. Slow progression of symptoms and LV remodelling in asymptomatic chronic primary MR was previously reported<sup>41</sup>. Finally, we chose not to exclude patients with AF since such condition is frequently encountered in primary MR. Although cine MRI and echocardiography can be more challenging in case of AF, such explorations remain fully interpretable and validated for MR evaluation. Indeed, most echocardiographic standardized methods to assess MR severity including EROA, which is considered as the most robust quantitative method, are not influenced by the presence of AF<sup>42</sup>. Beta blockers can alternately be used before the MRI exam in case of patients with rapid ventricular rate to optimize image quality.

## Conclusion

This study shows that new LA to mitral annulus angulation parameters, which were computed directly from available feature tracking-derived contours on standard-of-care MRI cine images, showed stronger, significant and independent associations with exercise capacity in patients with asymptomatic primary MR and preserved LVEF than commonly used parameters of cardiac function. Therefore, these parameters, which are driven by both annulus size and orientation as well as LA geometry, might complement existing flow and geometry parameters in MR severity grading.

## Data availability

The datasets used and/or analysed during the current study are available from the corresponding author on reasonable request.

Received: 14 December 2023; Accepted: 29 August 2024

Published online: 13 September 2024

## References

1. Iung, B. *et al.* Contemporary presentation and management of valvular heart disease. *Circulation* **140**, 1156–1169 (2019).
2. Enriquez-Sarano, M., Akins, C. W. & Vahanian, A. Mitral regurgitation. *Lancet* **373**, 1382–1394 (2009).
3. Vahanian, A. *et al.* 2021 ESC/EACTS Guidelines for the management of valvular heart disease. *Eur. Heart J.* **43**, 561–632 (2022).
4. Myerson, S. G. *et al.* Determination of clinical outcome in mitral regurgitation with Cardiovascular Magnetic Resonance quantification. *Circulation* **133**, 2287–2296 (2016).
5. Uretsky, S. *et al.* Discordance between echocardiography and MRI in the assessment of mitral regurgitation severity: A prospective multicenter trial. *J. Am. Coll. Cardiol.* **65**, 1078–1088 (2015).
6. Lamy, J. *et al.* Scan-rescan reproducibility of ventricular and atrial MRI feature tracking strain. *Comput. Biol. Med.* **92**, 197–203 (2018).
7. Fischer, K. *et al.* Feature tracking myocardial strain incrementally improves prognostication in myocarditis beyond traditional CMR imaging features. *JACC Cardiovasc. Imaging* **13**, 1891–1901 (2020).
8. Evin, M. *et al.* Assessment of left atrial function by MRI myocardial feature tracking. *J. Magn. Reson. Imaging* **42**, 379–389 (2015).
9. Kowallick, J. T. *et al.* Quantification of left atrial strain and strain rate using Cardiovascular Magnetic Resonance myocardial feature tracking: A feasibility study. *J. Cardiovasc. Magnetic Resonance* **16**, 60 (2014).
10. Chirinos, J. A. *et al.* Left atrial phasic function by Cardiac Magnetic Resonance feature tracking is a strong predictor of incident cardiovascular events. *Circ. Cardiovasc. Imaging* **11**, e007512 (2018).
11. Huber, A. T. *et al.* Cardiac MR strain: A noninvasive biomarker of fibrofatty remodeling of the left atrial myocardium. *Radiology* **286**, 83–92 (2017).
12. Tang, S.-S. *et al.* Additive effects of mitral regurgitation on left ventricular strain in essential hypertensive patients as evaluated by cardiac magnetic resonance feature tracking. *Front. Cardiovasc. Med.* **9**, 995366 (2022).
13. Lapinskas, T. *et al.* Left atrial mechanics in patients with acute STEMI and secondary mitral regurgitation: A prospective pilot CMR feature tracking study. *Medicina* **53**, 11–18 (2017).
14. Matsumori, M. *et al.* Efficacy of left atrial plication for atrial functional mitral regurgitation. *Gen. Thorac. Cardiovasc. Surg.* **69**, 458–465 (2021).
15. Al-Mohaissen, M. A., Chow, B. J. W., Lee, T. & Chan, K.-L. Left atrial-left ventricular angle, a new measure of left atrial and left ventricular remodeling. *Int. J. Cardiovasc. Imaging* **38**, 435–445 (2022).
16. Lancellotti, P. *et al.* Recommendations for the echocardiographic assessment of native valvular regurgitation: An executive summary from the European Association of Cardiovascular Imaging. *Eur. Heart J. Cardiovasc. Imaging* **14**, 611–644 (2013).
17. Myers, J. *et al.* Recommendations for clinical exercise laboratories: A scientific statement from the American Heart Association. *Circulation* **119**, 3144–3161 (2009).
18. Hammoudi, N. *et al.* Altered cardiac reserve is a determinant of exercise intolerance in sickle cell anaemia patients. *Eur. J. Clin. Investigation* **52**, e13664 (2022).
19. Herment, A. *et al.* Automated segmentation of the aorta from phase contrast MR images: Validation against expert tracing in healthy volunteers and in patients with a dilated aorta. *J. Magn. Reson. Imaging* **31**, 881–888 (2010).
20. Uretsky, S., Argulian, E., Narula, J. & Wolff, S. D. Use of cardiac magnetic resonance imaging in assessing mitral regurgitation. *J. Am. Coll. Cardiol.* **71**, 547–563 (2018).
21. Evin, M. *et al.* Left atrial aging: A cardiac magnetic resonance feature-tracking study. *Am. J. Physiol.-Heart Circ. Physiol.* **310**, H542–H549 (2016).
22. Soghomonian, A. *et al.* Is increased myocardial triglyceride content associated with early changes in left ventricular function? A 1H-MRS and MRI strain study. *Front. Endocrinol.* **14**, 1181452 (2023).
23. Yoganathan, T. *et al.* Acute stress induces long-term metabolic, functional, and structural remodeling of the heart. *Nat. Commun.* **14**, 3835 (2023).
24. Gottlieb, L. A. *et al.* Reduction in left atrial and pulmonary vein dimensions after ablation therapy is mediated by scar. *IJC Heart Vasculture* **37**, 100894 (2021).



25. Coisne, A. *et al.* Prognostic values of exercise echocardiography and cardiopulmonary exercise testing in patients with primary mitral regurgitation. *Eur. Heart J. Cardiovasc. Imaging* **23**, 1552–1561 (2022).
26. Messika-Zeitoun, D. *et al.* Cardiopulmonary exercise testing determination of functional capacity in mitral regurgitation: Physiologic and outcome implications. *J. Am. Coll. Cardiol.* **47**, 2521–2527 (2006).
27. Naji, P. *et al.* Importance of exercise capacity in predicting outcomes and determining optimal timing of surgery in significant primary mitral regurgitation. *J. Am. Heart Assoc.* **3**, e001010 (2014).
28. Izumo, M. *et al.* Changes in mitral regurgitation and left ventricular geometry during exercise affect exercise capacity in patients with systolic heart failure. *Eur. J. Echocardiogr.* **12**, 54–60 (2011).
29. Mentias, A. *et al.* Strain echocardiography and functional capacity in asymptomatic primary mitral regurgitation with preserved ejection fraction. *J. Am. Coll. Cardiol.* **68**, 1974–1986 (2016).
30. Alashi, A. *et al.* Synergistic utility of brain natriuretic peptide and left ventricular global longitudinal strain in asymptomatic patients with significant primary mitral regurgitation and preserved systolic function undergoing mitral valve surgery. *Circ. Cardiovasc. Imaging* **9**, e004451 (2016).
31. Yang, L.-T. *et al.* Effects of left atrial strain on functional capacity in chronic severe mitral regurgitation. *Int. J. Cardiol.* **168**, e151–e153 (2013).
32. Ahmed, M. I. *et al.* Increased oxidative stress and cardiomyocyte myofibrillar degeneration in patients with chronic isolated mitral regurgitation and ejection fraction >60%. *J. Am. Coll. Cardiol.* **55**, 671–679 (2010).
33. Seemann, F. *et al.* Valvular imaging in the era of feature-tracking: A slice-following cardiac MR sequence to measure mitral flow. *J. Magn. Reson. Imaging* **51**, 1412–1421 (2020).
34. Anwar, A. M., Geleijnse, M. L., Soliman, O. I. I., Nemes, A. & Cate, F. J. Left atrial Frank-Starling law assessed by real-time, three-dimensional echocardiographic left atrial volume changes. *Heart* **93**, 1393–1397 (2007).
35. Meyer, M., McEntee, R. K., Nyotowidjojo, I., Chu, G. & LeWinter, M. M. Relationship of exercise capacity and left ventricular dimensions in patients with a normal ejection fraction. An exploratory study. *PLoS ONE* **10**, e0119432 (2015).
36. Tischler, M. D., Niggel, J., Borowski, D. T. & LeWinter, M. M. Relation between left ventricular shape and exercise capacity in patients with left ventricular dysfunction. *J. Am. Coll. Cardiol.* **22**, 751–757 (1993).
37. Arena, R. *et al.* Ventilatory efficiency and resting hemodynamics in hypertrophic cardiomyopathy. *Med. Sci. Sports Exercise* **40**, 799–805 (2008).
38. Guazzi, M. *et al.* 2016 focused update: Clinical recommendations for cardiopulmonary exercise testing data assessment in specific patient populations. *Eur. Heart J.* **39**, 1144–1161 (2018).
39. Le Tourneau, T. *et al.* Echocardiography predictors and prognostic value of pulmonary artery systolic pressure in chronic organic mitral regurgitation. *Heart* **96**, 1311–1317 (2010).
40. Magne, J. *et al.* Impact of exercise pulmonary hypertension on postoperative outcome in primary mitral regurgitation. *Heart* **101**, 391–396 (2015).
41. Gaasch, W. H. & Meyer, T. E. Left ventricular response to mitral regurgitation: Implications for management. *Circulation* **118**, 2298–2303 (2008).
42. Zoghbi, W. *et al.* Recommendations for evaluation of the severity of native valvular regurgitation with two-dimensional and Doppler echocardiography. *J. Am. Soc. Echocardiogr.* **16**, 777–802 (2003).

## Acknowledgements

PM was funded by “Fondation Coeur & Artères—FCA 21T1”; MG was funded by Bureau de Bourse of Paris Republic of Djibouti Embassy (reference 654596/AMB/BGDEF/20-23 and 23-24); VN was funded by H2020 MAESTRIA (#965286).

## Author contributions

All authors contributed significantly to this manuscript. All authors: manuscript drafting or manuscript revision for important intellectual content. All authors: approval of final version of submitted manuscript. All authors: literature research. PM, TW, MG, EB, EC, AR, NH, NK: study concepts/study design or data acquisition or data and statistical analysis or findings interpretation. PM, MG, JL, VN, NK: software design for quantification and analysis.

## Competing interests

The authors declare no competing interests.

## Additional information

**Correspondence** and requests for materials should be addressed to N.K.

**Reprints and permissions information** is available at [www.nature.com/reprints](http://www.nature.com/reprints).

**Publisher’s note** Springer Nature remains neutral with regard to jurisdictional claims in published maps and institutional affiliations.

**Open Access** This article is licensed under a Creative Commons Attribution-NonCommercial-NoDerivatives 4.0 International License, which permits any non-commercial use, sharing, distribution and reproduction in any medium or format, as long as you give appropriate credit to the original author(s) and the source, provide a link to the Creative Commons licence, and indicate if you modified the licensed material. You do not have permission under this licence to share adapted material derived from this article or parts of it. The images or other third party material in this article are included in the article’s Creative Commons licence, unless indicated otherwise in a credit line to the material. If material is not included in the article’s Creative Commons licence and your intended use is not permitted by statutory regulation or exceeds the permitted use, you will need to obtain permission directly from the copyright holder. To view a copy of this licence, visit <http://creativecommons.org/licenses/by-nc-nd/4.0/>.

© The Author(s) 2024